DECIDUALIZATION INDUCES A SECRETOME SWITCH IN PERIVASCULAR NICHE CELLS OF THE HUMAN ENDOMETRIUM

Decidualization Induces a Secretome Switch in Perivascular Niche Cells of the Human Endometrium

Keisuke Murakami, Yie Hou Lee, Emma S. Lucas, Yi-Wah Chan, Ruban Peter Durairaj, Satoru Takeda, Jonathan D. Moore, Bee K. Tan, Siobhan Quenby, Jerry K. Y. Chan, Caroline E. Gargett, and Jan J. Brosens

Division of Reproductive Health, Clinical Science Research Laboratories (K.M., E.S.L., R.P.D., B.K.T., S.Q., J.J.B.), Warwick Medical School, University of Warwick, Coventry CV2 2DX, United Kingdom; Department of Obstetrics and Gynaecology (K.M., S.T.), Juntendo University Faculty of Medicine, Tokyo, 113-8421, Japan; Interdisciplinary Research Groups of BioSystems and Micromechanics, and Infectious Diseases (Y.H.L.), Singapore-MIT Alliance for Research and Technology, Singapore 138602; Warwick Systems Biology Centre (Y.-W.C., J.D.M.), University of Warwick, Coventry CV4 7AL, United Kingdom; Department of Reproductive Medicine (J.K.Y.C.), KK Women's and Children's Hospital, Singapore 229899; Cancer and Stem Cell Biology Program (J.K.Y.C.), Duke-NUS Graduate Medical School, Singapore, 169857; and The Ritchie Centre (C.E.G.), Monash Institute of Medical Research–Prince Henry's Institute, Institute of Medical Research and Department of Obstetrics and Gynaecology, Monash University, Clayton, 3168, Australia

The endometrial perivascular microenvironment is rich in mesenchymal stem-like cells that express type 1 integral membrane protein Sushi domain containing 2 (SUSD2) but the role of these cells in the decidual transformation of this tissue in pregnancy is unknown. We used an antibody directed against SUSD2 (W5C5) to isolate perivascular ($W5C5^+$) and nonperivascular ($W5C5^-$) fibroblasts from mid-luteal biopsies. We show that *SUSD2* expression, and hence the ratio of $W5C5^+$:$W5C5^-$ cells, changes in culture depending on cell-cell contact and activation of the Notch signaling pathway. RNA sequencing revealed that cultures derived from $W5C5^+$ progenitor cells remain phenotypically distinct by the enrichment of novel and established endometrial perivascular signature genes. In an undifferentiated state, $W5C5^+$-derived cells produced lower levels of various chemokines and inflammatory modulators when compared with their $W5C5^-$ counterparts. This divergence in secretomes was switched and became more pronounced upon decidualization, which transformed perivascular $W5C5^+$ cells into the dominant source of a range of chemokines and cytokines, including leukemia inhibitory factor and chemokine (C-C motif) ligand 7. Our findings suggest that the decidual response is spatially organized at the embryo-maternal interface with differentiating perivascular cells establishing distinct cytokine and chemokine profiles that could potentially direct trophoblast toward maternal vessels and govern local immune responses in pregnancy. **(*Endocrinology* 155: 4542–4553, 2014)**

The hallmark of the human reproductive cycle, shared only with a handful of other mammalian species, is menstruation, which is triggered by cyclic decidualization of the endometrium in response to endocrine rather than embryonic cues (1, 2). Decidualization, a process characterized by the transformation of stromal fibroblast into specialized secretory decidual cells, is driven by the post-ovulatory increase in circulating progesterone levels and increasing local cAMP production (3–5). Typically, it commences with the transformation of stromal cells surrounding spiral arterioles during the midluteal phase of the cycle and then spreads to encompass the whole superficial endometrial layer as the cycle progresses. Increasing evidence suggests that cyclic decidualization emerged as

ISSN Print 0013-7227 ISSN Online 1945-7170
Printed in U.S.A.

Received May 7, 2014. Accepted August 6, 2014.
First Published Online August 13, 2014

Abbreviations: HESC, human endometrial stromal cell; LIF, leukemia inhibitory factor; MACS, magnetic-activated cell sorting; MCAM, melanoma cell adhesion molecule; MPA, medroxyprogesterone acetate MSC, mesenchymal stem-like cell; PE, phycoerythrin; sST2, soluble ST2; SUSD2, Sushi domain containing 2.

an evolutionary strategy to cope with highly invasive and often chromosomally abnormal embryos (6). This conjecture is predicated on the observation that decidual cells selectively migrate toward high-quality human embryos and are capable of mounting a response that is tailored to individual embryos (6–8). In case of a developmentally competent embryo, decidual cells protect the conceptus against environmental stress signals (9, 10), confer maternal immunetolerance to the fetal allograft (11, 12), provide a nutritive matrix for trophoblast expansion (13, 14), and ensure tissue hemostasis during endovascular trophoblast invasion and spiral artery remodeling (15, 16). By contrast, signals emanating from developmentally impaired human embryos trigger a proteotoxic stress response in decidual cells, thus enabling prompt maternal recognition and rejection (6).

The decidual phenotype is inextricably linked to continuous progesterone signaling (17–20). Consequently, in the absence of a viable pregnancy, decreasing progesterone levels trigger a cascade of events that ultimately leads to proteolytic breakdown of the superficial endometrium and menstrual shedding. In the first few years after the menarche, 90% of all menstrual cycles are anovulatory, de facto ensuring that menstruation precedes pregnancy. This observation led to the suggestions that repeated cycles of tissue regeneration protects the uterus against tissue damage associated with deep hemorrhagic trophoblast invasion (21). Perhaps surprising, only over the last decade has the focus gradually turned on the role of endometrial progenitor/stem cells in effecting endometrial regeneration (22, 23). It is now established that the endometrium is rich in mesenchymal stem-like cells (MSCs) that are clonogenic, multipotent, immunoprivileged, and capable of reconstituting endometrium when xenotransplanted into mice (24–28). Several approaches have been employed to isolate endometrial stromal populations enriched in MSCs, including flow-activated cell sorting of side population cells that possess a low Hoechst 33342 fluorescence profile and of cells that coexpress cluster of differentiation 140b (CD140b, platelet-derived growth factor receptor β) and CD146 (also known as melanoma cell adhesion molecule, [MCAM]) (29, 30). Recent studies reported that the monoclonal antibody W5C5 selectively binds a stromal cell population enriched in MSCs in both bone marrow and endometrium (31, 32). Subsequently, the type 1 integral membrane protein Sushi domain containing 2 (SUSD2) was identified as the cognate antigen for W5C5 (33). Like $CD140b^+CD146^+$stromal cells, $W5C5^+$/SUSD2 expressing cells surround the spiral arteries throughout the endometrium. Based on analysis of 56 midluteal endometrial biopsies and 34 hysterectomy samples from all cycle stages, $W5C5^+$ cells were found to make up on average 6.8% and 4.2% of stromal cells, respectively (32, 34). Colony-forming cells make up a small proportion of $W5C5^+$ and $W5C5^-$ cells. In the hysterectomy samples, the abundance of clonogenic cells in the $W5C5^+$ cell fraction was 3.6% (range, 0.7–6.9) whereas the frequency in the $W5C5^-$ cell population was only 0.2% (range, 0–1.2) (32). Analysis of midluteal biopsies confirmed the marked enrichment of colony-forming cells in the $W5C5^+$ cell fraction (34).

In this study, we demonstrate that *SUSD2* is a downstream target of the Notch-signaling pathway, which in turn accounts for density-dependent homeostatic balancing of $W5C5^+$ and $W5C5^-$ cells in culture irrespective of the parental stromal cell population. However, we also show that $W5C5^+$-derived cells retain phenotypic features of perivascular niche cells when propagated in culture and mount a decidual response that is highly divergent from the bulk of endometrial stromal cells.

Materials and Methods

Human endometrial tissue collection

The study was approved by the National Health Service National Research Ethics–Hammersmith and Queen Charlotte's & Chelsea Research Ethics Committee (1997/5065). Subjects were recruited from the Implantation Clinic, a dedicated research clinic at University Hospitals Coventry and Warwickshire National Health Service Trust. Written informed consent was obtained from all participants in accordance with the guidelines in The Declaration of Helsinki 2000. Samples were obtained using a Wallach Endocell sampler (Wallach) under ultrasound guidance, starting from the uterine fundus and moving downward to the internal cervical ostium. A total of 43 subjects took part in this study. Endometrial biopsies were timed between 6–10 days after the preovulatory LH surge. All biopsies were obtained in ovulatory cycles and none of the subjects were on hormonal treatments for at least 3 months prior to the procedure. The average age ($\pm$ SEM) of the participants was 35.2 $\pm$ 0.7 years.

Isolation of $W5C5^+$ and $W5C5^-$ cells and primary cell culture

Single-cell suspensions of human endometrial stromal cells (HESCs) were isolated from midluteal biopsies as previously described (32, 34), albeit with several modifications. Briefly, samples were washed in DMEM/F-12 medium (Invitrogen), finely minced, and enzymatically digested with collagenase (0.5 mg/ml; SigmaAldrich) and deoxyribonuclease (DNase) type I (0.1 mg/ml; Roche) for 1 hour at 37°C. The dissociated cells were filtered through a 40-μm cell strainer (Fisher Scientific). Stromal cells and blood cells, present as a single-cell suspension, passed through the cell strainer, whereas the undigested fragments, mostly comprising glandular clumps, were retained on the strainer. Stromal single-cell suspensions were layered over Ficoll-Paque PLUS (GE Healthcare) and centrifuged to remove erythrocytes. The medium/Ficoll-Paque PLUS interface, containing stromal cells, was carefully aspirated, washed with DMEM/F-12

medium, and then subjected to magnetic bead separation to isolate W5C5$^+$ and W5C5$^-$ cells as described previously (32, 34). Briefly, freshly isolated HESC suspensions (up to 1×10^6 cells/100 μl of Magnetic Bead buffer consisting of 0.5% BSA in PBS) were incubated with phycoerythrin (PE) conjugated antihuman W5C5 (SUSD2) antibody (5 μl/1×10^6 cells; BioLegend) on ice for 20 minutes. Cell suspensions (up to 1×10^7 cells/80 μl of Magnetic Bead buffer) were then incubated with anti-PE-magnetic-activated cell sorting MicroBeads (20 μl/1×10^7 cells; Miltenyi Biotec) on ice for 20 minutes. Cell suspensions (up to 1×10^8 cells/500 μl of Magnetic Bead buffer) were applied onto MS columns (Miltenyi Biotec) in a magnetic field, followed by washing with 500 μl of Magnetic Bead buffer three times. Although W5C5$^-$ cells passed through the column, magnetically labeled W5C5$^+$ cells were retained on the column. The columns were removed from the magnetic field and W5C5$^+$ cells were flushed with 1 ml of Magnetic Bead buffer. Cell counts after magnetic separation allowed calculation of the percentage of W5C5$^+$ and W5C5$^-$ cells. Freshly isolated W5C5$^+$ and W5C5$^-$ cells were expanded in growth medium consisting of DMEM/F12 with 10% dextran-coated charcoal-treated fetal bovine serum, 1% L-glutamine (Invitrogen), 1% antibiotic-antimycotic solution (Invitrogen), insulin (2 μg/ml; SigmaAldrich), estradiol (1 nM; SigmaAldrich), and basic fibroblast growth factor (10 ng/ml; Merck Millipore). For repeat separation experiments, confluent W5C5$^+$ and W5C5$^-$ cell cultures were trypsinized and relabeled with PE antihuman W5C5 antibody and anti-PE-magnetic-activated cell sorting MicroBeads, as described above.

Differentiation experiments were carried out at passage 2. Briefly, confluent W5C5$^+$ and W5C5$^-$ cell cultures were incubated in phenol red-free DMEM/F12 containing 2% dextran-coated charcoal-treated fetal bovine serum, 1% antibiotic-antimycotic solution, 0.5mM 8-bromoadenosine cAMP (8-bromo-cAMP; SigmaAldrich) and 1μM medroxyprogesterone acetate (MPA; SigmaAldrich). The medium was changed every 48 hours. For cell cycle experiments, unsorted HESCs were seeded in six-well plates, maintained in growth medium overnight, and then incubated in serum-free medium for 24 hours to synchronize the cells. Trypan blue exclusion test showed negligent decline in cell viability (average 2.4%) upon serum deprivation. After 24 hours, cells were reincubated in growth medium and re-entered the cell cycle. Total RNA was collected at different time points. To examine the involvement of Notch signaling, primary HESCs were seeded at the density of 20 000 cells/cm^2 and then maintained in growth medium supplemented with or without the γ secretase inhibitor DAPT (10μM; SigmaAldrich). The cultures were expanded for 4 days and then either collected for total RNA or subjected to magnetic-activated cell sorting (MACS) as described above. The cumulative loss of HESC viability over the treatment period in response to exposure to DAPT was 7.4%.

Immunocytochemistry

Immunocytochemistry was performed using W5C5$^+$- and W5C5$^-$-derived cell cultures. Cells were fixed with 4% paraformaldehyde (SigmaAldrich) for 30 minutes and blocked with 3% BSA/5% normal goat serum in PBS for 30 minutes. Cells were then incubated with an antihuman SUSD2 antibody (1:400; SigmaAldrich) for 1 hour at room temperature. The secondary antibody used was Alexa Fluor 488 (1:200; Invitrogen). Slides were mounted with VECTASHIELD and stained with 4′,6-diamidino-2-phenylindole (DAPI) to visualize nuclei. Images were captured using a Zeiss Laser Scanning Microscope LSM 510.

RNA-sequencing and data analysis

Total RNA from passage 2 cultures was extracted using RNA STAT-60 (AMS Biotechnology) following the manufacturer's protocol, including DNase treatment (Invitrogen). RNA quality was analyzed on an Agilent 2100 Bioanalyser (Agilent Technologies) and assessed with the Eukaryotic Total RNA Nano program according to the manufacturer's instructions. RNA integrity number score for all samples was at least 9. Transcriptomic alignments were identified using bowtie-0.12.8 (35), samtools-0.1.18, and tophat-2.0.4 (36) against the University of California Santa Cruz hg19 reference transcriptome from the Illumina iGenomes resource. Gene counts were estimated using HTSeq-0.5.3p3 (http://www-huber.embl.de/users/anders/HTSeq/). Transcripts per million were calculated as recently described (37). Count data from the TopHat-HTSeq pipeline were analyzed using three different methods for differential expression detection, ie, DESeq, baySeq, and edgeR (38–40). Gene transcript abundances between W5C5$^+$ and W5C5$^-$ were considered significantly different if the false discovery rate value (baySeq and edgeR) or adjusted P value (DESeq) was $< .01$. Differentially expressed genes were retained if they were detected by at least two of the methods used. Sequence data have been submitted to GEO (GSE57182).

qRT-PCR

Total RNA was extracted from freshly isolated or cultured W5C5$^+$ cells and W5C5$^-$ cells using RNA STAT-60. Equal amounts of total RNA were treated with DNase and reverse transcribed by using the QuantiTect Reverse Transcription Kit (QIAGEN) and the resulting cDNA was used as template in qRT-PCR analysis. Template quantification was performed with Power SYBR Green PCR Master Mix and the 7500 real-time PCR System (Applied Biosystems). The expression levels of the samples were expressed as arbitrary units defined by the $\Delta\Delta$CT method. The variances of input cDNA were normalized against the levels of the *L19* housekeeping gene. All measurements were performed in triplicate. Melting curve analysis and agarose gel electrophoresis confirmed amplification specificity. The gene-specific primer pairs were designed using Primer3 software. The primer sequences are listed in Supplemental Material 1.

Western blot analysis

Whole cell protein extracts were prepared by lysing cells in Radioimmunoprecipitation assay buffer (Merck Millipore) containing protease inhibitors (Complete Mini, Roche). Protein yield was quantified using the Bio-Rad protein assay (Bio-Rad, Hemel Hempstead). Equal amounts of proteins were separated by SDS-PAGE and transferred to polyvinylidene fluoride membrane (GE Healthcare). Nonspecific binding sites were blocked by overnight incubation with 5% nonfat dry milk in tris-buffered saline with 0.1% Tween-20. The membranes were then probed with antibodies raised against SUSD2 (PE antihuman W5C5 [SUSD2] antibody, BioLegend, diluted 1:500); and β-actin (SigmaAldrich, diluted 1:100 000). After incubation with horseradish peroxidase-conjugated secondary antibodies, protein complexes were visualized with the Enhanced Chemiluminescence Plus Western-Blotting Detection Reagents (GE Healthcare).

Secretome analysis

For these experiments, 2×10^5 W5C5$^-$- or W5C5$^+$-derived cells were plated per well in six-well plates and decidualized when confluent. Undiluted conditioned medium from undifferentiated and differentiated W5C5$^+$ and W5C5$^-$ selected cultures was assayed for 48 cytokines, chemokines, and growth factors, listed in Supplemental Material 2, using a multiplex suspension bead immunoassay (Bio-Rad) according to manufacturer's instructions. Data analysis of experimental data was carried out using five-parameter logistic regression modeling on the Bio-Plex system. Soluble ST2 (sST2) levels were determined using an amplified two-step sandwich-type immunoassay (DuoSet; R&D Systems) according to the manufacturer's protocol. Results were derived using the standard curve method.

Statistical analysis

All statistical analyses were performed using GraphPad Prism 6 (GraphPad Software) and EZR software (Easy R). Data were checked for normal distribution using histograms and the Shapiro-Wilk test. Unpaired *t* test, paired *t* test, or Wilcoxon signed-rank test was performed to determine statistical significance between groups. When comparing three or more groups, the data were analyzed using ANOVA test followed by the *t* test with Bonferroni adjustment. $P < .05$ was considered significant.

Results

Isolation and culturing of W5C5$^+$ and W5C5$^-$ HESCs

To characterize the constituent fibroblast populations of the endometrial stromal compartment, single-cell suspensions were prepared from midluteal biopsies and separated into W5C5$^+$ and W5C5$^-$ cell fractions by magnetic-activated cell sorting (MACS). qRT-PCR and Western blot analysis confirmed that freshly isolated W5C5$^+$ cells are highly enriched in *SUSD2* mRNA (9-fold) and protein expression when compared to W5C5$^-$ cells (Figure 1A). However, this difference in SUSD2 expression was not maintained when W5C5$^+$ and W5C5$^-$ cells were expanded in culture (Figure 1B). To

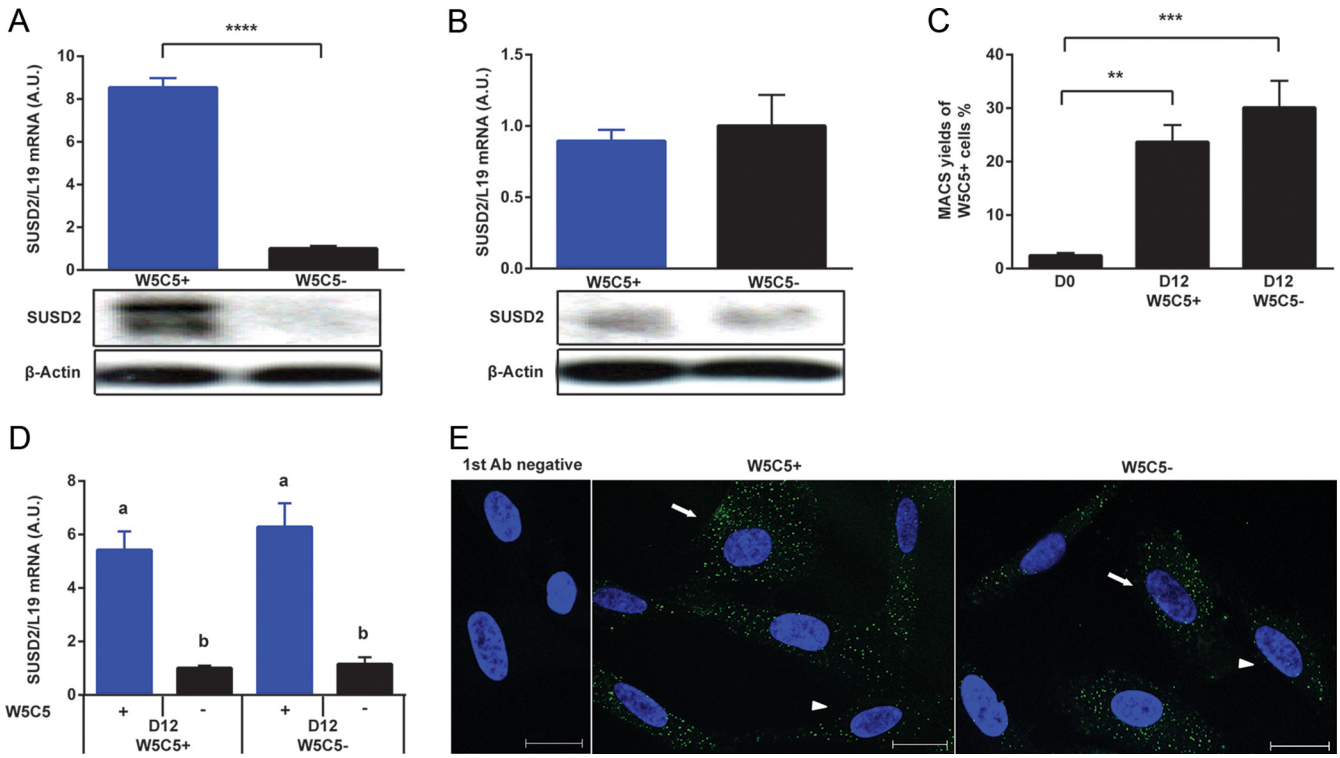

Figure 1. Characterization of W5C5/SUSD2-positive and -negative cells in culture. A, *SUSD2* expression was determined at mRNA and protein level in freshly isolated W5C5$^+$ and W5C5$^-$ cells by qRT-PCR and Western blot analysis, respectively. Transcript levels are expressed in arbitrary units (AU). β-Actin served as loading control for Western blot analysis. Data represent mean ± SEM of three biological repeat experiments. ****, $P < .0001$. B, SUSD2 expression was also assessed in cultured W5C5$^+$ and W5C5$^-$ cells by qRT-PCR and Western blot analysis. Data represent mean ± SEM of three biological repeat experiments. C, W5C5$^+$ and W5C5$^-$ cells cultured for 12 days were subjected to reselection using W5C5 antibody. The MACS yields of W5C5$^+$ cells were 2.4 ± 0.5% in fresh samples. The abundance of W5C5$^+$ cells upon reselection of cultured W5C5$^+$- and W5C5$^-$-derived cells was 23.7 ± 3.2% and 30.1 ± 5.0%, respectively. Data represent mean ± SEM of six biological repeat experiments. ***, $P < .001$; **, $P < .01$. D, SUSD2 mRNA expression in W5C5$^+$ cells and W5C5$^-$ cells reseparated from cultured W5C5$^+$ or W5C5$^-$ cells. Data represent mean ± SEM of three biological repeat experiments. Different letters above error bars indicate that those groups are significantly different from each other at $P < .05$. E, W5C5$^+$ and W5C5$^-$ cells maintained in culture were immunolabeled for SUSD2 (green) and nuclei visualized with DAPI (blue). Confocal microscopy revealed a mixture of strongly (arrow) and weakly (arrowhead) SUSD2 immunoreactive cells in both W5C5$^+$- and W5C5$^-$-derived cultures. Scale bar, 20 μm.

investigate this further, we subjected cultured W5C5$^+$ and W5C5$^-$ cells to reselection using the W5C5 antibody. As shown in Figure 1C, only 23.7 ± 3.2% of cells were still positive after culturing purified W5C5$^+$ cells for 12 days. Even more unexpectedly, 30.1 ± 5.0% of originally W5C5$^-$ cells became positive upon culturing for 12 days. After repeat MACS, *SUSD2* mRNA expression was much higher in the W5C5$^+$ cell fraction, irrespective of the culture being derived from W5C5$^+$ or W5C5$^-$ parental cells (Figure 1D). In agreement, SUSD2 immunostaining was indistinguishable between cultures established from W5C5$^+$ or W5C5$^-$ stromal cell fractions (Figure 1E). Taken together, these data point toward homeostatic balancing of W5C5/SUSD2-positive and -negative cell populations, at least under in vitro cultures. Furthermore, while W5C5/SUSD2-positive cells make up between 4.2–6.8% of freshly isolated HESCs (32, 34), their abundance increases markedly in culture, irrespective of the level of *SUSD2* expression in progenitor cells.

SUSD2 expression is regulated by Notch signaling

We hypothesized that *SUSD2* expression in HESCs could be cell-cycle dependent, thus accounting for homeostatic balancing of W5C5/SUSD2-positive and -negative cell populations in culture. To test this hypothesis, we synchronized HESCs in G1 by serum starvation and monitored the transcript levels of *SUSD2* and various cell cycle markers upon refeeding with growth medium. As expected, resumption of the cell cycle resulted in sequential up-regulation of *CCND1* (G1/S phase), *MYBL2* (S phase), and *CCNB1* (G2/M phase) expression. By contrast, *SUSD2* mRNA levels remained constant throughout, indicating that expression is not cell-cycle dependent (Figure 2A). Next we investigated whether *SUSD2* expression is dependent on cell-cell signaling. Primary HESCs were seeded at low (group A, 400 cells/cm^2), intermediate (group B, 3000 cells/cm^2) or high (group C, 20 000 cells/cm^2) densities. After 4 days in growth culture, cells were counted and collected for mRNA analysis or subjected to repeat MACS. The average cell density (± SEM) at harvesting was 11 300 ± 1243 cells/cm^2 for group A, 71 300 ± 9237 cells/cm^2 for group B, and 127 900 ± 9107 cells/cm^2 for group C. Increasing cell density correlated with higher expression levels of *SUSD2* mRNA (Figure 2B); and increased W5C5$^+$:W5C5$^-$ ratio (Figure 2C).

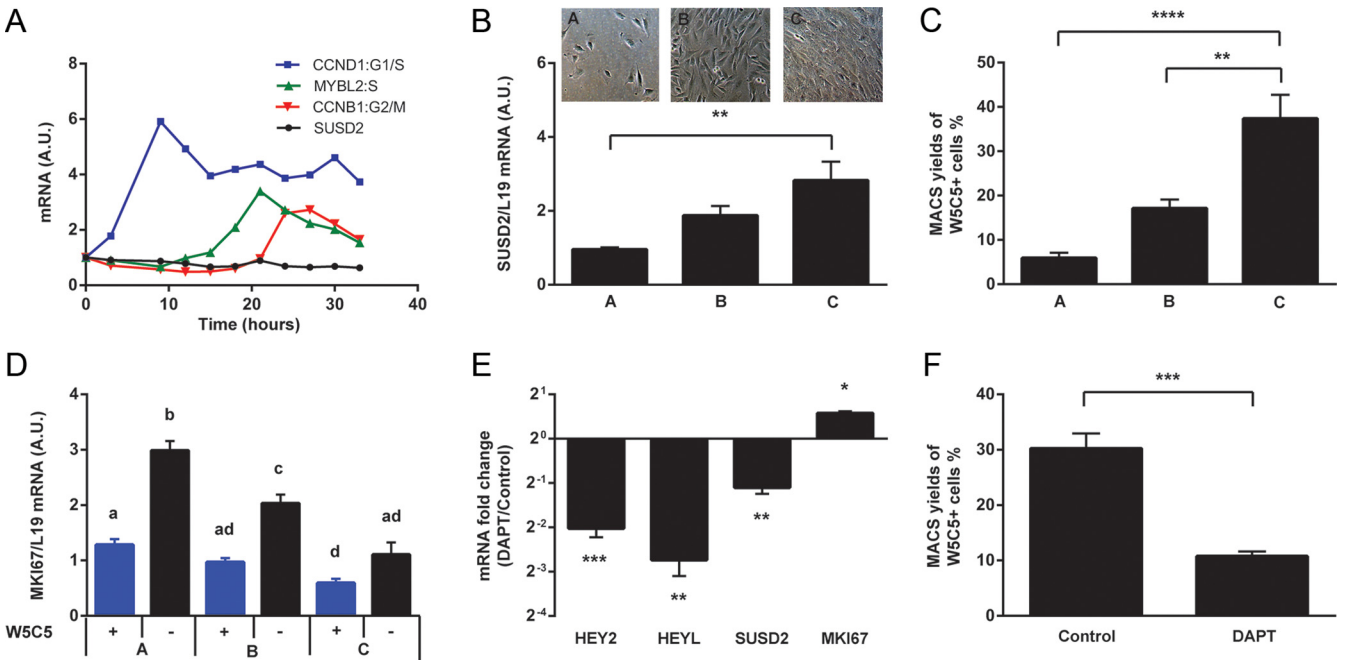

Figure 2. *SUSD2* is regulated by Notch signaling. A, Unselected primary HESCs were synchronized in G1 by serum starvation for 24 hours and then reincubated in growth medium and collected at the indicated time points. Expression of *SUSD2* and various cell cycle markers were assessed by qRT-PCR. B, Primary HESCs were seeded at low (group A), intermediate (group B), or high (group C) densities. The cultures were expanded for 4 days and then collected for qRT-PCR. C, Parallel cultures were subjected to repeat MACS using the W5C5 antibody. Data represent mean ± SEM of five biological repeat experiments. ****, $P < .0001$; **, $P < .01$. D, Total RNA was extracted from reselected W5C5$^+$ and W5C5$^-$ cells and proliferative activity assessed by measuring *MKI67* transcript levels. Data represent mean ± SEM of five biological repeat experiments. Different letters above error bars indicate that those groups are significantly different from each other at $P < .05$. E, Primary HESCs were grown to confluence over 4 days in the presence or absence of DAPT, an inhibitor of the Notch pathway. Total RNA was then extracted and subjected to qRT-PCR analysis. The data show relative change in transcript levels in response to DAPT exposure. Note the log^2 scale of the y-axis. Data represent mean ± SEM of five biological repeat experiments. ***, $P < .001$; **, $P < .01$; *, $P < .05$. F, Parallel cultures were subjected to repeat MACS to assess the impact of Notch inhibition on the abundance of W5C5$^+$ cells. Data represent mean ± SEM of five biological repeat experiments.

The expression of *MKI67*, encoding the proliferation marker Ki-67 antigen, correlated inversely with the density of either W5C5$^+$ or W5C5$^-$ cells (Figure 2D), reflecting that HESCs exhibit contact inhibition of growth. Notably, *MKI67* mRNA levels were consistently higher in W5C5$^-$ compared with W5C5$^+$ cells independent of culture density.

The apparent dependency of *SUSD2* expression on cell-cell contact suggested possible involvement of Notch signaling. To test this hypothesis, we first measured expression of the Notch target genes *HEY1*, *HEY2*, and *HEYL* in reseparated W5C5$^+$ and W5C5$^-$ cells. Although there was no difference in *HEY1* expression, *HEY2* and *HEYL* transcript levels were significantly higher in the W5C5$^+$ cell population (Supplemental Figure 1). Next, we examined the affect of Notch inhibition on expression of *SUSD2* and the abundance of W5C5$^+$ cells. Primary HESCs were grown to confluence over 4 days in the presence or absence of the γ-secretase inhibitor DAPT. As shown in Figure 2D, abrogating Notch signaling in unselected HESCs down-regulated the expression of *HEY2* and *HEYL* transcripts while modestly up-regulating *MKI67* mRNA expression (Figure 2E). Importantly, Notch inhibition down-regulated *SUSD2* mRNA expression by 53% and, concomitantly, reduced the abundance of W5C5$^+$ cells by 64%. Taken together, these data show that *SUSD2* is a downstream target gene in the Notch pathway in HESCs (Figure 2F).

Gene signatures of cultured W5C5$^+$- and W5C5$^-$-derived cells

The failure of SUSD2/W5C5 marker to differentiate between cultured HESC subpopulations raised the possibility that W5C5$^+$ and W5C5$^-$ cells revert to a similar basal phenotype when propagated in vitro. To test this hypothesis, we established W5C5$^+$ and W5C5$^-$ cultures from four midluteal biopsies and profiled the transcriptomes by RNA sequencing. On average, 22 million single-end reads were sequenced per sample. Of 18 985 expressed genes, 101, 77, and 901 were identified as significantly different between W5C5$^+$ and W5C5$^-$ cultures by baySeq, DESeq, and edgeR differential expression analyses, respectively. Combining these analyses, we identified a robust list of 134 differentially expressed genes detected by at least two methods (Figure 3A; Supplemental Tables 1 and 2). To assess further the relatedness of the cultures, we calculated *z* scores of the transcripts-per-million values for the differentially expressed genes. A heat map of this association is depicted in Figure 3B. To test whether cultured W5C5$^+$ cells retain any in vivo phenotypic markers, we examined the endometrial tissue distribution of all differentially expressed genes using The Human Protein Atlas (http://www.proteinatlas.org/). We successfully annotated 115 of 134 genes and identified 12 that shared the same restricted tissue distribution as SUSD2, characterized by prominent immunostaining around endometrial arterioles (Supplemental Figure 2). Notable endometrial perivascular markers enriched in cultures originating from W5C5$^+$ cells included *NOTCH3*, *MCAM* (CD146), *AOC3* (vascular adhesion protein-1, also known as semicarbazide-sensitive amine oxidase), *ELN* (elastin), and *MYH11* (myosin-11, a smooth muscle myosin; Figure 3C, left panel). We further mined the RNA-sequencing data for expression of established MSC or pericyte markers, including *NT5E* (CD73), *ENG* (CD105), *ITGA5* (CD49e), *ALCAM* (CD166), *CD44* (CD44), *ITGB1* (CD29), *THY1* (CD90), and *PDGFRB* (CD140b). None of these surface markers were significantly enriched at transcript level in W5C5$^+$-derived cells (Figure 3C, right panel). However, mining of the extended edgeR data set suggested that W5C5$^+$-derived cultures also express higher levels of desmin (*DES*), alpha smooth muscle actin (*ACTA2*), as well as chondroitin sulfate proteoglycan 4 (*CSPG4*), which is implicated in pericyte recruitment and sprouting during angiogenesis (41, 42). Thus, whereas the expression of the W5C5 antigen *SUSD2* is regulated by culture conditions, W5C5$^+$-derived cells retain gene signatures of perivascular niche cells.

Decidualization of cultured W5C5$^+$- and W5C5$^-$-derived cells

We speculated that endometrial perivascular cells are programmed to mount a distinct decidual response in pregnancy. To explore this possibility, subconfluent W5C5$^+$ and W5C5$^-$-derived primary cultures were treated with 8-br-cAMP and MPA for 2, 4, or 8 days. Multiple-log increases in *PRL* and *HSD11B1* expression, key decidual marker genes (43), were observed in all differentiating cultures (Figure 4A and B). Further, the relative responsiveness to deciduogenic signals (ie, fold induction of marker genes) did not differ between W5C5$^-$ and W5C5$^+$-derived cells, although both basal as well as induced *PRL* and *HSD11B1* mRNA levels were consistently lower in the latter. *SUSD2* mRNA levels did not change significantly upon decidualization of either HESC subpopulation (Figure 4C). In keeping with the RNA-sequencing data, W5C5$^+$-derived cells expressed much higher *AOC3* mRNA levels compared with their W5C5$^-$ counterparts, irrespective of their differentiation status (Figure 4D). However, whereas the *AOC3* transcript levels remained constant upon decidualization of W5C5$^+$-derived cells, a biphasic pattern was observed in non-perivascular decidualizing cells with levels peaking around 4 days of differentiation. We also measured the

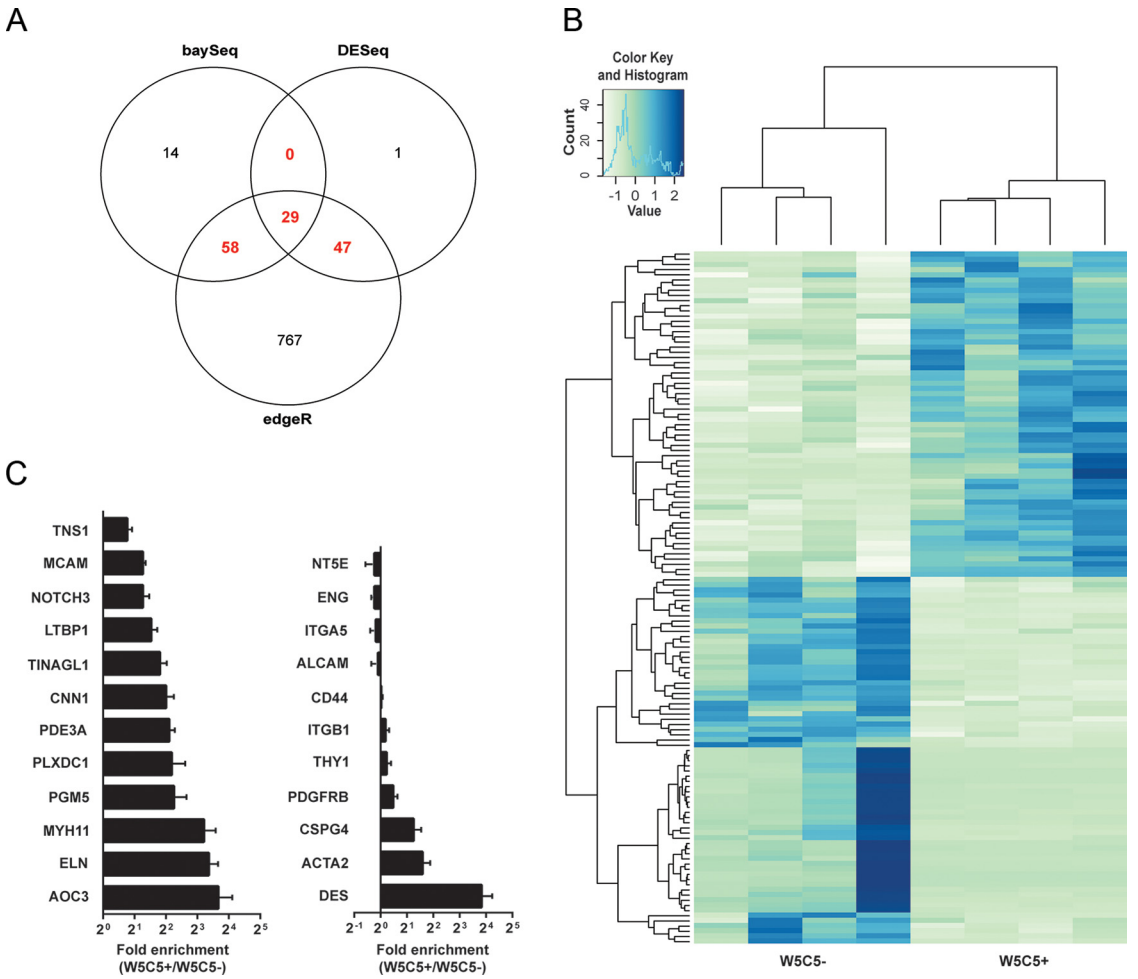

Figure 3. Cultured W5C5$^+$ cells express perivascular niche gene signatures. A, Venn diagram comparison of differentially expressed transcripts identified by baySeq, edger, and DESeq. Numbers represent transcripts with nonzero counts in four paired W5C5$^+$ and W5C5$^-$ cell cultures. B, Clustered heat map of top-ranked differentially expressed transcripts in primary cultures established from W5C5$^+$ or W5C5$^-$ cells. C, Pairwise analysis of the RNA-sequencing data showing fold enrichment in W5C5$^+$-derived cells of novel endometrial perivascular markers (left panel) as well as commonly used MSC and pericyte markers (right panel). Data represent mean ± SEM. Note the log^2 scale of the x-axis.

transcript levels for *IL33*, a key regulator of endometrial receptivity genes and innate immune responses (44), as well as the secreted levels of the IL-33 soluble decoy receptor sST2. Strikingly, *IL33* mRNA expression was consistently higher in the differentiating W5C5$^+$-derived cells whereas secreted anti-inflammatory sST2 levels were significantly higher in nonperivascular cells decidualized for 4 or 8 days (Figure 4, E and F). Taken together, these observations suggest that the decidual response is divergent between perivascular and nonperivascular cell populations in the endometrial stroma.

Next we examined whether the divergent expression profile of *IL-33* and sST2 in decidualizing W5C5$^-$ and W5C5$^+$-derived cells extends to other secreted factors. Of 48 immunomodulating factors measured by multiplex suspension bead immunoassay, 43 were detectable in conditioned medium of undifferentiated HESCs. Interestingly, nine factors (M-CSF, IL-6, IL-8, and 6 chemokines) were differentially secreted with levels being invariably higher in undifferentiated W5C5$^-$-derived primary cultures (Figure 5A; Supplemental Table 3). Decidualization was associated with increased secretion of 14 and 23 factors in W5C5$^-$ and W5C5$^+$-derived cultures, respectively (Supplemental Table 4). Consequently, the difference in secretome became much more pronounced upon decidualization, with W5C5$^+$-derived cells now producing significantly higher levels of 12 factors (Figure 5B; Supplemental Table 5). Notably, W5C5$^+$-derived cells continued to secrete lower levels of CXCL1, CXCL10, CCL5, IL-6, and IL-8 compared with their W5C5$^-$-derived counterparts whether decidualized or not. Partial least squares regression analysis allowed visualization of the divergent secretomes of decidualizing W5C5$^-$ and W5C5$^+$-derived cells (Figure 5C). Although the secretome profiles of undecidualized W5C5$^+$ and W5C5$^-$ cells formed a tight cluster, the shift upon decidualization was more pronounced in the perivascular W5C5$^+$-derived cell population.

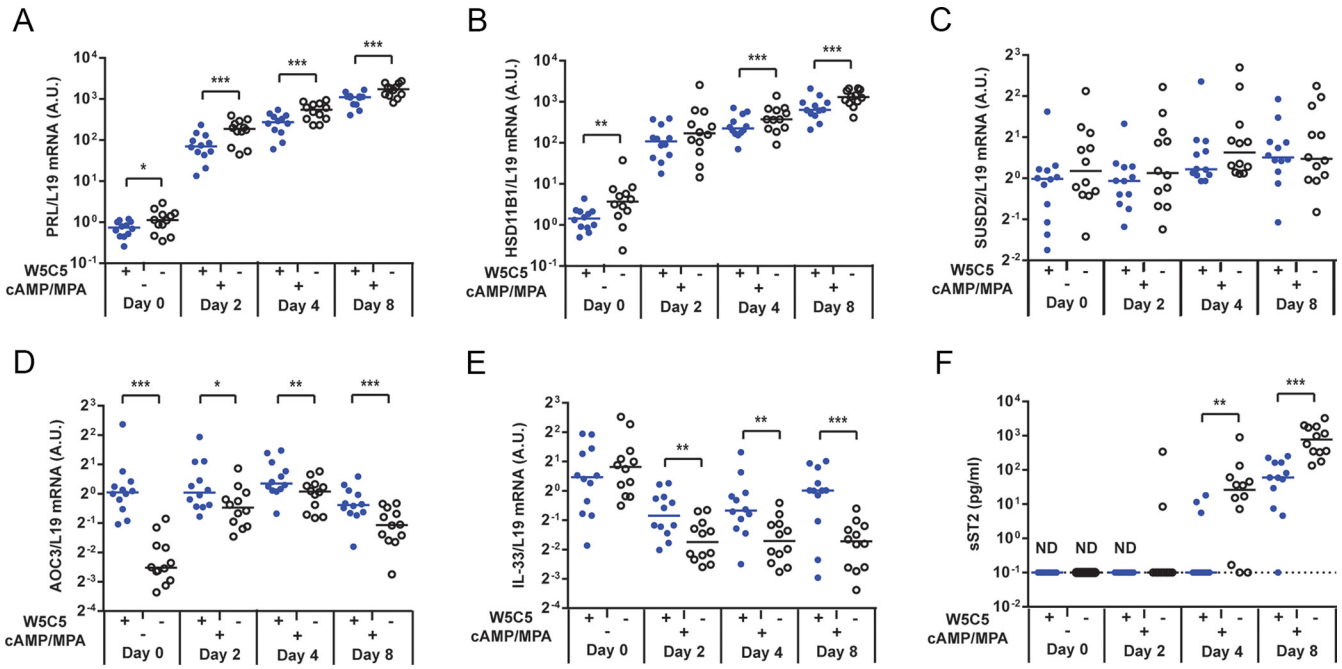

Figure 4. Divergent decidual response in W5C5$^-$ and W5C5$^+$-derived cells. W5C5$^+$ and W5C5$^-$ cells were isolated from 12 different midluteal endometrial biopsies, passaged twice in culture and then treated with or without 8-br-cAMP and MPA for 2, 4, or 8 days. The induction of highly sensitive decidual marker genes, A, *PRL*; and B, *HSD11B1* was examined by qRT-PCR. In addition, C, *SUSD2;* D, *AOC3;* and E, *IL33* transcript levels were also measured. Furthermore, the culture supernatants were assayed for F, the soluble IL-33 decoy receptor sST2 . Note that y-axis scale is $\log^{10}$ in A, B, and F; and $\log^2$ in C, D, and E. ***, $P < .001$; **, $P < .01$; and *, $P < .05$. ND, not detected.

Discussion

Most adult tissues contain resident stem cells, which compensate for physiological cell attrition and enable regeneration in response to tissue damage (45). The human endometrium is rather remarkable because it exhibits physiological tissue injury that leads to cyclic disposal and renewal of its superficial layer at menstruation. A parsimonious explanation for cyclic menstruation is that it bestows plasticity on the uterus through constant recruitment and/or activation of stem cells, which in turn may be key to accommodate intense tissue remodeling associated with deep placentation (46). In this respect, it is notable that there is a correlation between the extent of spontaneous decidualization, the amount of menstrual tissue shedding, and the depth of endovascular trophoblast invasion in menstruating mammals, with human beings far outperforming other primates (47–49).

It is widely accepted that the properties and potential of adult stem cells are defined by a combination of intrinsic characteristics and a tissue-specific microenvironment (50, 51). In the endometrium, the perivascular space around the rapidly growing spiral arterioles constitutes an important regulatory niche, presumably consisting of both quiescent and active MSCs, transient amplifying cells, and neighboring nonstem cells. In this study, we demonstrate that freshly isolated SUSD2 expressing endometrial fibroblast are perivascular cells programmed to mount a distinctive decidual response. SUSD2 is a recently identified 820 amino acid protein consisting of a large extracellular region containing various motifs involved in cell-cell and cell-matrix adhesion (52–54). This type I transmembrane protein was shown to accumulate on the plasma membrane of bone marrow MSCs at the site of cell-cell contact (33). Similarly, we found that its expression, both at transcript and protein level, increases markedly upon direct cell-cell contact in both W5C5$^+$- and W5C5$^-$-derived cultures. Depending on the cellular context, SUSD2 has been implicated in growth inhibition as well as the enhancement of the metastatic potential of cancer cells (52–54). In endometrial stromal cells, *SUSD2* expression is responsive to Notch activation and associated with proliferation inhibition. High Notch activity is a common niche feature essential for cell-fate specification and maintenance of stem cells in a poised quiescent state (45, 55). For example, silencing of Notch signaling in skeletal stem cells leads to premature activation, prevents the return to the quiescent state, and gives rise to muscles that lack the ability to regenerate in response to injury (55). By analogy, it seems plausible that pathological cues arising from dysmetabolic conditions associated with adverse pregnancy outcome, such as obesity, interfere with Notch signaling in the endometrium, thus gradually depleting the tissue of quiescent stem cells and rendering it vulnerable to damage in pregnancy (34). Interestingly, a previous mi-

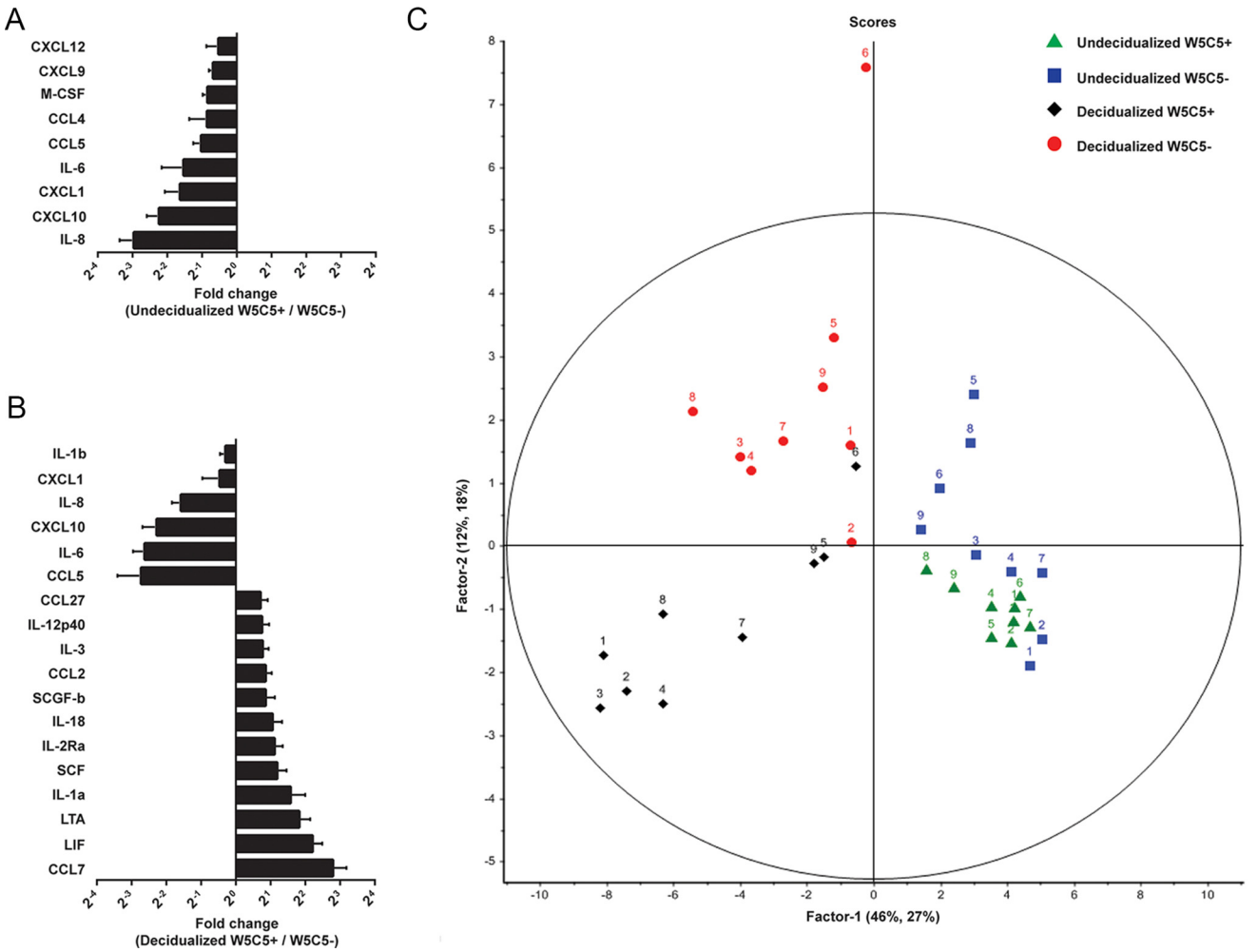

Figure 5. Secretome analysis of decidualizing W5C5$^+$- and W5C5$^-$-derived cells. A, The secretion of 48 inflammatory mediators was measured by multiplex suspension bead immunoassay in paired undifferentiated W5C5$^+$ and W5C5$^-$ cultures. Nondecidualized perivascular niche cells secrete lower levels of several immune modulators when compared with undifferentiated W5C5$^-$-derived cells. B, However, upon decidualization, W5C5$^+$-derived cells are more active and produce higher levels of 12 decidual immune molecules. Data represent mean ± SEM of nine biological repeat experiments. C, Two-dimensional partial least squares loadings plot of W5C5$^+$ and W5C5$^-$ secretomes in undifferentiated and decidualized states.

croarray study reported only modestly raised (approximately 2-fold) *SUSD2* transcript in freshly isolated perivascular CD140b$^+$CD146$^+$ MSCs when compared with CD140b$^+$CD146$^-$ stromal fibroblasts (30). Conversely, pairwise analysis revealed that *MCAM* mRNA (coding CD146) is only marginally higher in W5C5$^+$cells, which contrasts with the 10-fold difference in transcript levels between CD140b$^+$CD146$^+$ and CD140b$^+$CD146$^-$ cells. Nevertheless, 19 of 63 genes (30%) enriched in cultured W5C5$^+$-derived cells are also enriched in freshly isolated CD140b$^+$CD146$^+$MSCs (annotated in Supplemental Table 1), indicating close kinship between these subpopulations although their precise functions within the endometrial perivascular niche await further elucidation.

Notch signaling plays a major role in establishing transcriptional memory (56). Our study yielded ample evidence that cell identity is partly maintained when different endometrial stromal subpopulations are expanded vastly in culture. As aforementioned, RNA sequencing of cultured undifferentiated cells identified 12 novel marker genes reflecting the perivascular origins of W5C5$^+$-derived cells. We also show that undifferentiated perivascular cells express lower levels of *PRL* and *HSD11B1*, yet the relative induction of these differentiation genes in response to deciduogenic signals was comparable to that observed in nonperivascular stromal cells. The quality of the decidual response, however, was strikingly divergent. For example, human primary amine oxidase (AOC3), also known as vascular adhesion protein 1 or semicarbazide-sensitive amine oxidase, is a key inflammatory mediator because of its involvement in leukocyte trafficking (57). In nonperivascular decidualizing cells, the pattern of *AOC3* expression was identical to that of other proinflammatory mediators, characterized by rapid induction followed by

down-regulation as the differentiation process unfolds (44). In W5C5$^+$-derived cells, however, expression was both significantly higher and unresponsive to differentiation signals. Similarly, down-regulation of *IL33* transcript levels and reciprocal secretion of the IL-33 soluble decoy receptor sST2 was much more blunted in W5C5$^+$- compared with W5C5$^-$-derived cells. The most conspicuous evidence of a divergent differentiation response came from the secretome analysis, which showed that decidualization transforms the relatively quiescent perivascular cells into a dominant source of 12 immunomodulators and trophic factors. For example, the secretion of chemokine (C-C motif) ligand 7 (CCL7, formerly monocyte chemotactic protein-3 or MCP-3) increased 43-fold upon decidualization of perivascular cells but only 5-fold in W5C5$^-$-derived stromal cell cultures. CCL7 is a highly promiscuous chemokine capable of attracting monocytes as well as lymphocytes, granulocytes, NK cells, and dendritic cells (58, 59). Similarly, basal leukemia inhibitory factor (LIF) secretion was comparable between different cultures but the levels increased 18-fold and 4-fold upon decidualization of W5C5$^+$- and W5C5$^-$-derived cells, respectively. LIF is a multifaceted cytokine indispensible for embryo implantation and decidualization (60, 61). Importantly, LIF also functions as a chemoattractant for human trophoblast and promotes differentiation toward the invasive extravillous trophoblast phenotype (62, 63).

Taken together, these observations suggest that *SUSD2*-expressing perivascular cells establish specific chemokine profiles around the uterine vessels. Although as yet untested, a distinct perivascular microenvironment in early pregnancy may serve to coordinate immune cell trafficking at the feto-maternal interface and promote endovascular trophoblast invasion, a process essential for the transformation of low-capacity, high-resistance spiral arteries into high-capacity, low-resistance vessels that can sustain placental function in the later stages of pregnancy (1, 64, 65). If so, functional analysis of the perivascular decidual response prior to conception could potentially identify women at risk of placental disorders in pregnancy, such as fetal growth restriction and preeclampsia. Additional studies are warranted to test this possibility.

Acknowledgments

Address all correspondence and requests for reprints to: Jan Brosens, MD, PhD, Division of Reproductive Health, Clinical Science Research Laboratories, Warwick Medical School, University of Warwick, Coventry CV2 2DX, United Kingdom. E-mail: j.j.brosens@warwick.ac.uk.

This work was supported by the Biomedical Research Unit in Reproductive Health, a joint initiative between the University Hospitals Coventry and Warwickshire National Health Service Trust and Warwick Medical School. C.E.G. also received funding from The Australian National Health and Medical Research Council for a Senior Research Fellowship 1042298 and the Victorian Government's Operational Infrastructure Support Program. The funders had no role in study design, data collection and analysis, decision to publish, or preparation of the article.

Disclosure Summary: The authors have nothing to disclose.

References

1. **Brosens JJ, Pijnenborg R, Brosens IA.** The myometrial junctional zone spiral arteries in normal and abnormal pregnancies: A review of the literature. *Am J Obstet Gynecol*. 2002;187:1416–1423.
2. **Emera D, Romero R, Wagner G.** The evolution of menstruation: a new model for genetic assimilation: explaining molecular origins of maternal responses to fetal invasiveness. *Bioessays*. 2012;34:26–35.
3. **Brosens JJ, Hayashi N, White JO.** Progesterone receptor regulates decidual prolactin expression in differentiating human endometrial stromal cells. *Endocrinology*. 1999;140:4809–4820.
4. **Gellersen B, Brosens J.** Cyclic AMP and progesterone receptor cross-talk in human endometrium: A decidualizing affair. *J Endocrinol*. 2003;178:357–372.
5. **Jones MC, Fusi L, Higham JH, et al.** Regulation of the SUMO pathway sensitizes differentiating human endometrial stromal cells to progesterone. *Proc Natl Acad Sci USA*. 2006;103:16272–16277.
6. **Brosens JJ, Salker MS, Teklenburg G, et al.** Uterine selection of human embryos at implantation. *Sci Rep*. 2014;4:3894.
7. **Teklenburg G, Salker M, Molokhia M, et al.** Natural selection of human embryos: Decidualizing endometrial stromal cells serve as sensors of embryo quality upon implantation. *PLoS One*. 2010;5:e10258.
8. **Weimar CH, Kavelaars A, Brosens JJ, et al.** Endometrial stromal cells of women with recurrent miscarriage fail to discriminate between high- and low-quality human embryos. *PLoS One*. 2012;7:e41424.
9. **Kajihara T, Jones M, Fusi L, et al.** Differential expression of FOXO1 and FOXO3a confers resistance to oxidative cell death upon endometrial decidualization. *Mol Endocrinol*. 2006;20:2444–2455.
10. **Leitao B, Jones MC, Fusi L, et al.** Silencing of the JNK pathway maintains progesterone receptor activity in decidualizing human endometrial stromal cells exposed to oxidative stress signals. *Faseb J*. 2010;24:1541–1551.
11. **Nancy P, Tagliani E, Tay CS, Asp P, Levy DE, Erlebacher A.** Chemokine gene silencing in decidual stromal cells limits T cell access to the maternal-fetal interface. *Science*. 2012;336:1317–1321.
12. **Zhang S, Lin H, Kong S, et al.** Physiological and molecular determinants of embryo implantation. *Mol Aspects Med*. 2013;34:939–980.
13. **Gonzalez M, Neufeld J, Reimann K, et al.** Expansion of human trophoblastic spheroids is promoted by decidualized endometrial stromal cells and enhanced by heparin-binding epidermal growth factor-like growth factor and interleukin-1 β. *Mol Hum Reprod*. 2011;17:421–433.
14. **Grewal S, Carver JG, Ridley AJ, Mardon HJ.** Implantation of the human embryo requires Rac1-dependent endometrial stromal cell migration. *Proc Natl Acad Sci USA*. 2008;105:16189–16194.
15. **Lockwood CJ, Krikun G, Rahman M, Caze R, Buchwalder L, Schatz F.** The role of decidualization in regulating endometrial hemostasis during the menstrual cycle, gestation, and in pathological states. *Semin Thromb Hemost*. 2007;33:111–117.

16. **Lockwood CJ, Paidas M, Murk WK, et al.** Involvement of human decidual cell-expressed tissue factor in uterine hemostasis and abruption. *Thromb Res*. 2009;124:516–520.
17. **Evans J, Salamonsen LA.** Decidualized human endometrial stromal cells are sensors of hormone withdrawal in the menstrual inflammatory cascade. *Biol Reprod*. 2014;90:14.
18. **Finn CA, Pope M.** Vascular and cellular changes in the decidualized endometrium of the ovariectomized mouse following cessation of hormone treatment: A possible model for menstruation. *J Endocrinol*. 1984;100:295–300.
19. **Henriet P, Gaide Chevronnay HP, Marbaix E.** The endocrine and paracrine control of menstruation. *Mol Cell Endocrinol*. 2012;358:197–207.
20. **Labied S, Kajihara T, Madureira PA, et al.** Progestins regulate the expression and activity of the Forkhead transcription factor FOXO1 in differentiating human endometrium. *Mol Endocrinol*. 2006;20:35–44.
21. **Brosens JJ, Parker MG, McIndoe A, Pijnenborg R, Brosens IA.** A role for menstruation in preconditioning the uterus for successful pregnancy. *Am J Obstet Gynecol*. 2009;200:615 e611–616.
22. **Chan RW, Schwab KE, Gargett CE.** Clonogenicity of human endometrial epithelial and stromal cells. *Biol Reprod*. 2004;70:1738–1750.
23. **Schwab KE, Chan RW, Gargett CE.** Putative stem cell activity of human endometrial epithelial and stromal cells during the menstrual cycle. *Fertil Steril*. 2005;84 Suppl 2:1124–1130.
24. **Gargett CE, Ye L.** Endometrial reconstruction from stem cells. *Fertil Steril*. 2012;98:11–20.
25. **Miyazaki K, Maruyama T, Masuda H, et al.** Stem cell-like differentiation potentials of endometrial side population cells as revealed by a newly developed in vivo endometrial stem cell assay. *PLoS One*. 2012;7:e50749.
26. **Masuda H, Maruyama T, Hiratsu E, et al.** Noninvasive and real-time assessment of reconstructed functional human endometrium in NOD/SCID/gamma c(null) immunodeficient mice. *Proc Natl Acad Sci USA*. 2007;104:1925–1930.
27. **Wolff EF, Wolff AB, Hongling Du, Taylor HS.** Demonstration of multipotent stem cells in the adult human endometrium by in vitro chondrogenesis. *Reprod Sci*. 2007;14:524–533.
28. **Wolff EF, Gao XB, Yao KV, et al.** Endometrial stem cell transplantation restores dopamine production in a Parkinson's disease model. *J Cell Mol Med*. 2011;15:747–755.
29. **Schwab KE, Gargett CE.** Co-expression of two perivascular cell markers isolates mesenchymal stem-like cells from human endometrium. *Hum Reprod*. 2007;22:2903–2911.
30. **Spitzer TL, Rojas A, Zelenko Z, et al.** Perivascular human endometrial mesenchymal stem cells express pathways relevant to self-renewal, lineage specification, and functional phenotype. *Biol Reprod*. 2012;86:58.
31. **Bühring HJ, Battula VL, Treml S, Schewe B, Kanz L, Vogel W.** Novel markers for the prospective isolation of human MSC. *Ann N Y Acad Sci*. 2007;1106:262–271.
32. **Masuda H, Anwar SS, Bühring HJ, Rao JR, Gargett CE.** A novel marker of human endometrial mesenchymal stem-like cells. *Cell Transplant*. 2012;21:2201–2214.
33. **Sivasubramaniyan K, Harichandan A, Schumann S, et al.** Prospective isolation of mesenchymal stem cells from human bone marrow using novel antibodies directed against Sushi domain containing 2. *Stem Cells Dev*. 2013;22:1944–1954.
34. **Murakami K, Bhandari H, Lucas ES, et al.** Deficiency in clonogenic endometrial mesenchymal stem cells in obese women with reproductive failure - a pilot study. *PLoS One*. 2013;8:e82582.
35. **Langmead B, Trapnell C, Pop M, Salzberg SL.** Ultrafast and memory-efficient alignment of short DNA sequences to the human genome. *Genome Biol*. 2009;10:R25.
36. **Trapnell C, Pachter L, Salzberg SL.** TopHat: Discovering splice junctions with RNA-Seq. *Bioinformatics*. 2009;25:1105–1111.
37. **Wagner GP, Kin K, Lynch VJ.** Measurement of mRNA abundance using RNA-seq data: RPKM measure is inconsistent among samples. *Theory Biosci*. 2012;131:281–285.
38. **Anders S, Huber W.** Differential expression analysis for sequence count data. *Genome Biol*. 2010;11:R106.
39. **Hardcastle TJ, Kelly KA.** baySeq: Empirical Bayesian methods for identifying differential expression in sequence count data. *BMC Bioinformatics*. 2010;11:422.
40. **Robinson MD, McCarthy DJ, Smyth GK.** edgeR: A Bioconductor package for differential expression analysis of digital gene expression data. *Bioinformatics*. 2010;26:139–140.
41. **Fukushi J, Makagiansar IT, Stallcup WB.** NG2 proteoglycan promotes endothelial cell motility and angiogenesis via engagement of galectin-3 and alpha3beta1 integrin. *Mol Biol Cell*. 2004;15:3580–3590.
42. **Cattaruzza S, Nicolosi PA, Braghetta P, et al.** NG2/CSPG4-collagen type VI interplays putatively involved in the microenvironmental control of tumour engraftment and local expansion. *J Mol Cell Biol*. 2013;5:176–193.
43. **Kuroda K, Venkatakrishnan R, Salker MS, et al.** Induction of 11β-HSD 1 and activation of distinct mineralocorticoid receptor- and glucocorticoid receptor-dependent gene networks in decidualizing human endometrial stromal cells. *Mol Endocrinol*. 2013;27:192–202.
44. **Salker MS, Nautiyal J, Steel JH, et al.** Disordered IL-33/ST2 Activation in Decidualizing Stromal Cells Prolongs Uterine Receptivity in Women with Recurrent Pregnancy Loss. *PLoS One*. 2012;7:e52252.
45. **Cheung TH, Rando TA.** Molecular regulation of stem cell quiescence. *Nat Rev Mol Cell Biol*. 2013;14:329–340.
46. **Blanks AM, Brosens JJ.** Meaningful menstruation: Cyclic renewal of the endometrium is key to reproductive success. *Bioessays*. 2013;35:412.
47. **Finn CA.** Menstruation: A nonadaptive consequence of uterine evolution. *Q Rev Biol*. 1998;73:163–173.
48. **Martin RD.** The evolution of human reproduction: A primatological perspective. *Am J Phys Anthropol*. 2007;Suppl 45:59–84.
49. **Ramsey EM, Houston ML, Harris JW.** Interactions of the trophoblast and maternal tissues in three closely related primate species. *Am J Obstet Gynecol*. 1976;124:647–652.
50. **Fuchs E, Tumbar T, Guasch G.** Socializing with the neighbors: Stem cells and their niche. *Cell*. 2004;116:769–778.
51. **Scadden DT.** Nice Neighborhood: Emerging Concepts of the Stem Cell Niche. *Cell*. 2014;157:41–50.
52. **Sugahara T, Yamashita Y, Shinomi M, et al.** von Willebrand factor type D domain mutant of SVS-1/SUSD2, vWD(m), induces apoptosis in HeLa cells. *Cancer Sci*. 2007;98:909–915.
53. **Sugahara T, Yamashita Y, Shinomi M, et al.** Isolation of a novel mouse gene, mSVS-1/SUSD2, reversing tumorigenic phenotypes of cancer cells in vitro. *Cancer Sci*. 2007;98:900–908.
54. **Watson AP, Evans RL, Egland KA.** Multiple functions of sushi domain containing 2 (SUSD2) in breast tumorigenesis. *Mol Cancer Res*. 2013;11:74–85.
55. **Bjornson CR, Cheung TH, Liu L, Tripathi PV, Steeper KM, Rando TA.** Notch signaling is necessary to maintain quiescence in adult muscle stem cells. *Stem Cells*. 2012;30:232–242.
56. **Lake RJ, Tsai PF, Choi I, Won KJ, Fan HY.** RBPJ, the major transcriptional effector of Notch signaling, remains associated with chromatin throughout mitosis, suggesting a role in mitotic bookmarking. *PLoS Genet*. 2014;10:e1004204.
57. **Jalkanen S, Salmi M.** VAP-1 and CD73, endothelial cell surface enzymes in leukocyte extravasation. *Arterioscler Thromb Vasc Biol*. 2008;28:18–26.
58. **Rollins BJ.** Chemokines. *Blood*. 1997;90:909–928.
59. **Menten P, Wuyts A, Van Damme J.** Monocyte chemotactic protein-3. *Eur Cytokine Netw*. 2001;12:554–560.
60. **Shuya LL, Menkhorst EM, Yap J, Li P, Lane N, Dimitriadis E.**

Leukemia inhibitory factor enhances endometrial stromal cell decidualization in humans and mice. *PLoS One*. 2011;6:e25288.

61. **Stewart CL, Kaspar P, Brunet LJ, et al.** Blastocyst implantation depends on maternal expression of leukaemia inhibitory factor. *Nature*. 1992;359:76–79.
62. **Gellersen B, Wolf A, Kruse M, Schwenke M, Bamberger AM.** Human Endometrial Stromal Cell-Trophoblast Interactions: Mutual Stimulation of Chemotactic Migration and Pro-Migratory Roles of Cell Surface Molecules CD82 and CEACAM1. *Biol Reprod*. 2013; 88:80.
63. **Tapia A, Salamonsen LA, Manuelpillai U, Dimitriadis E.** Leukemia inhibitory factor promotes human first trimester extravillous trophoblast adhesion to extracellular matrix and secretion of tissue inhibitor of metalloproteinases-1 and -2. *Hum Reprod*. 2008;23: 1724–1732.
64. **Brosens I, Pijnenborg R, Vercruysse L, Romero R.** The "Great Obstetrical Syndromes" are associated with disorders of deep placentation. *Am J Obstet Gynecol*. 2011;204:193–201.
65. **Brosens I, Robertson WB, Dixon HG.** The physiological response of the vessels of the placental bed to normal pregnancy. *J Pathol Bacteriol*. 1967;93:569–579.